Ocean temperature response to idealized Gleissberg and de Vries solar cycles in a comprehensive climate model

Anne Seidenglanz,[1] Matthias Prange,[1] Vidya Varma,[1] and Michael Schulz[1]

Received 21 August 2012; revised 15 October 2012; accepted 17 October 2012; published 17 November 2012.

[1] The ∼90-year Gleissberg and ∼200-year de Vries cycles have been identified as two distinctive quasi-periodic components of Holocene solar activity. Evidence exists for the impact of such multi-decadal to centennial-scale variability in total solar irradiance (TSI) on climate, but concerning the ocean, this evidence is mainly restricted to the surface response. Here we use a comprehensive global climate model to study the impact of idealized solar forcing, representing the Gleissberg and de Vries cycles, on global ocean potential temperature at different depth levels, after a recent proxy record indicates a signal of TSI anomalies in the northeastern Atlantic at mid-depth. Potential impacts of TSI anomalies on deeper oceanic levels are climatically relevant due to their possible effect on ocean circulation by altering water mass characteristics. Simulated solar anomalies are shown to penetrate the ocean down to at least deep-water levels. Despite the fact that the two forcing periods differ only by a factor of ∼2, the spatial pattern of response is significantly distinctive between the experiments, suggesting different mechanisms for solar signal propagation. These are related to advection by North Atlantic Deep Water flow (200-year forcing), and barotropic adjustment in the South Atlantic in response to a latitudinal shift of the westerly wind belt (90-year forcing). **Citation:** Seidenglanz, A., M. Prange, V. Varma, and M. Schulz (2012), Ocean temperature response to idealized Gleissberg and de Vries solar cycles in a comprehensive climate model, *Geophys. Res. Lett.*, *39*, L22602, doi:10.1029/2012GL053624.

1. Introduction

[2] Variations in total solar irradiance (TSI) on multi-decadal to centennial time scales may constitute an important contribution to climate variability on a societal time scale and have been widely discussed [e.g., *Gray et al.*, 2010]. Reconstructions of TSI based on cosmogenic radionuclides have identified the Gleissberg (∼90 years) and de Vries (∼200 years) cycles as two distinctive quasi-periodic and non-stationary components in Holocene solar activity [*Knudsen et al.*, 2009; *Ma*, 2009]. Evidence of the surface climatic and oceanic response to solar impact on these time scales has been inferred from variations in sea surface temperature [e.g., *Bond et al.*, 2001; *Jiang et al.*, 2005], precipitation [e.g., *Wang et al.*, 2005], and variations in sea level pressure and associated wind fields [*Shindell et al.*, 2001; *Varma et al.*, 2011]. However, indications for the influence of solar anomalies on deeper oceanic levels is scarce.

[3] A correlation between foraminiferal Mg/Ca and TSI over the past 1200 years in the eastern North Atlantic is indicative for a propagation of solar-induced temperature anomalies also to sub-surface depths (900 m) [*Morley et al.*, 2011]. According to this study, temperature anomalies may propagate from the subpolar into the subtropical gyre in response to changes in solar-induced variations in surface wind forcing. Furthermore, numerical experiments with idealized solar forcing have been carried out, revealing sensitivity of the Atlantic Meridional Overturning Circulation (AMOC) to TSI changes on the multi-decadal to centennial time scale [*Park and Latif*, 2012].

[4] To address the oceanic response to TSI variations, we use a comprehensive global climate model. Sensitivity experiments with idealized solar forcing, representing the Gleissberg and de Vries solar cycles, are used to study the impact of multi-decadal to centennial-scale solar variability on ocean potential temperature at different depth levels. Spatial variability in the temperature response to this idealized forcing is interpreted in terms of propagation pathways of solar anomalies within the ocean. Contrary to previous studies, which aimed at simulating the true temperature response to the full range of solar variability during parts of the Holocene [e.g., *Cubasch et al.*, 1997; *Weber et al.*, 2004; *Ammann et al.*, 2007], this study focuses on the mechanisms of ocean response to idealized TSI at distinctive periods which have been detected in paleoclimatic records. Specifically, we address the following questions: (1) Is there a significant response in ocean temperature at the imposed forcing frequencies? (2) Can solar-induced changes in temperature be tracked to sub-surface depth in accordance with the proxy results? (3) What are the pathways of solar signal transfer into the oceanic interior?

2. Experimental Design

[5] Sensitivity experiments with idealized solar forcing were carried out using the NCAR Community Climate System Model Version 3 (CCSM3), a comprehensive global climate model consisting of ocean, atmosphere, land and sea-ice components [*Collins et al.*, 2006]. The CCSM3 has successfully been employed in earlier studies regarding the climate response to the 11-year solar cycle [*Meehl et al.*, 2008]. Considering the long integration time, the low resolution version with T31 spectral truncation [*Yeager et al.*, 2006] has been used. It corresponds to an atmospheric grid spacing of 3.75° and 26 levels in the vertical. The ocean model (POP) grid is resolved at 3.6° with a low-latitudinal refinement in resolution (maximum of 0.9° at the equator)

[1]MARUM–Center for Marine Environmental Sciences and Department of Geosciences, University of Bremen, Bremen Germany.

Corresponding author: A. Seidenglanz, MARUM–Center for Marine Environmental Sciences, University of Bremen, Leobener Straße, D-28359 Bremen Germany. (a.seidenglanz@uni-bremen.de)

0094-8276/12/2012GL053624

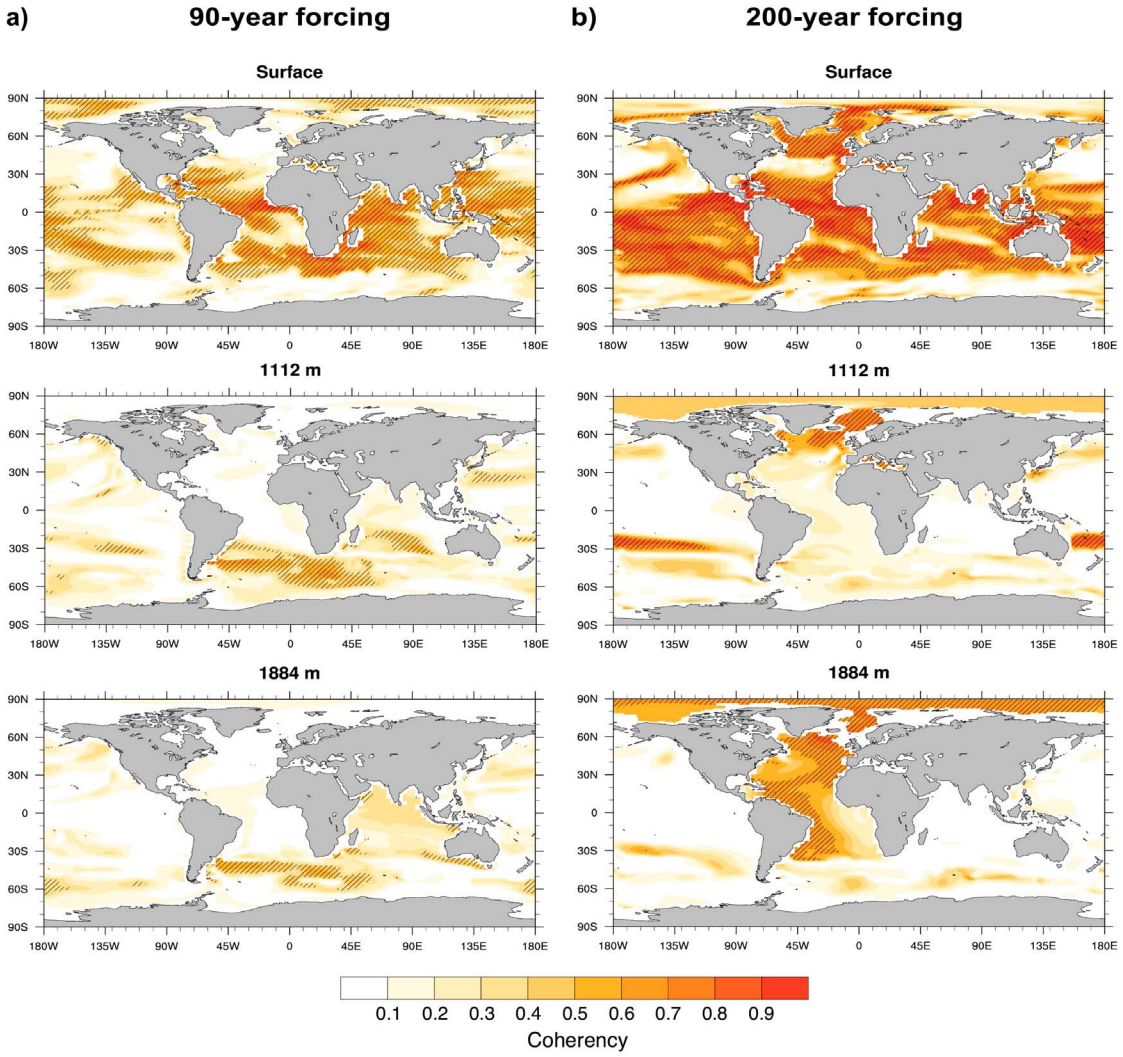

Figure 1. Coherency between ocean potential temperature (annual means) and TSI at the forcing periods of (a) 90 years (representing the Gleissberg cycle) and (b) 200 years (representing the de Vries cycle), for three depth levels. Hatching indicates significant values at the 95% level. Critical values of coherency are 0.34 and 0.59 in the 90-year and in the 200-year forcing experiment, respectively.

and 25 levels. The stratosphere in the CCSM3 has only a low vertical resolution and does not include potential feedbacks associated with changes in stratospheric ozone due to solar UV (ultraviolet) variability [cf. *Krivova et al.*, 2011]. Solar forcing is implemented through a wavelength-independent change in TSI, hence mostly affects the climate system through shortwave absorption by the surface.

[6] Two sensitivity experiments with idealized TSI, each integrated for 1000 years, were carried out. Solar forcing varies sinusoidally with an amplitude of 1 Wm^{-2} (between 1364 Wm^{-2} and 1366 Wm^{-2}) at the periods of the Gleissberg cycle (90 years) and the de Vries cycle (200 years). This forcing amplitude corresponds to a maximum estimate of solar variations at multi-decadal to centennial time scales [e.g., *Steinhilber et al.*, 2009] and has been chosen to enhance the detectability in the model experiments. We note, however, that substantial uncertainty regarding the magnitude of past centennial-scale TSI variability exists [e.g., *Lockwood*, 2011]. To be comparable to each other, the two experiments were initialized from a quasi-equilibrated experiment with late Holocene (2.5 ka BP) orbital forcing, as the integration of the 200-year solar forcing experiment is a continuation of a previously performed 700-year long simulation with late Holocene boundary conditions [*Varma et al.*, 2011]. Pre-industrial conditions were applied for the atmospheric composition [*Braconnot et al.*, 2007].

[7] The impact of TSI anomalies on the global oceanic temperature field is studied by means of cross-spectral analysis. (Squared) coherency between solar forcing and annual means of temperature time series is determined at the two forcing periods (90 and 200 years), and at specified depth levels, in order to identify regions of significant impact of TSI anomalies on ocean temperature. This is extended by studying the lag of the temperature response to TSI forcing at the two forcing periods to conclude about possible propagation pathways of solar anomalies within the ocean. The phase angle (ϕ) is defined in the interval [$-180°$; $+180°$] due to the periodic behavior of the arcus-tangent function. The phase angle is converted into a corresponding phase lag (τ) using $\tau = \phi / 360° \cdot T$, where T denotes the

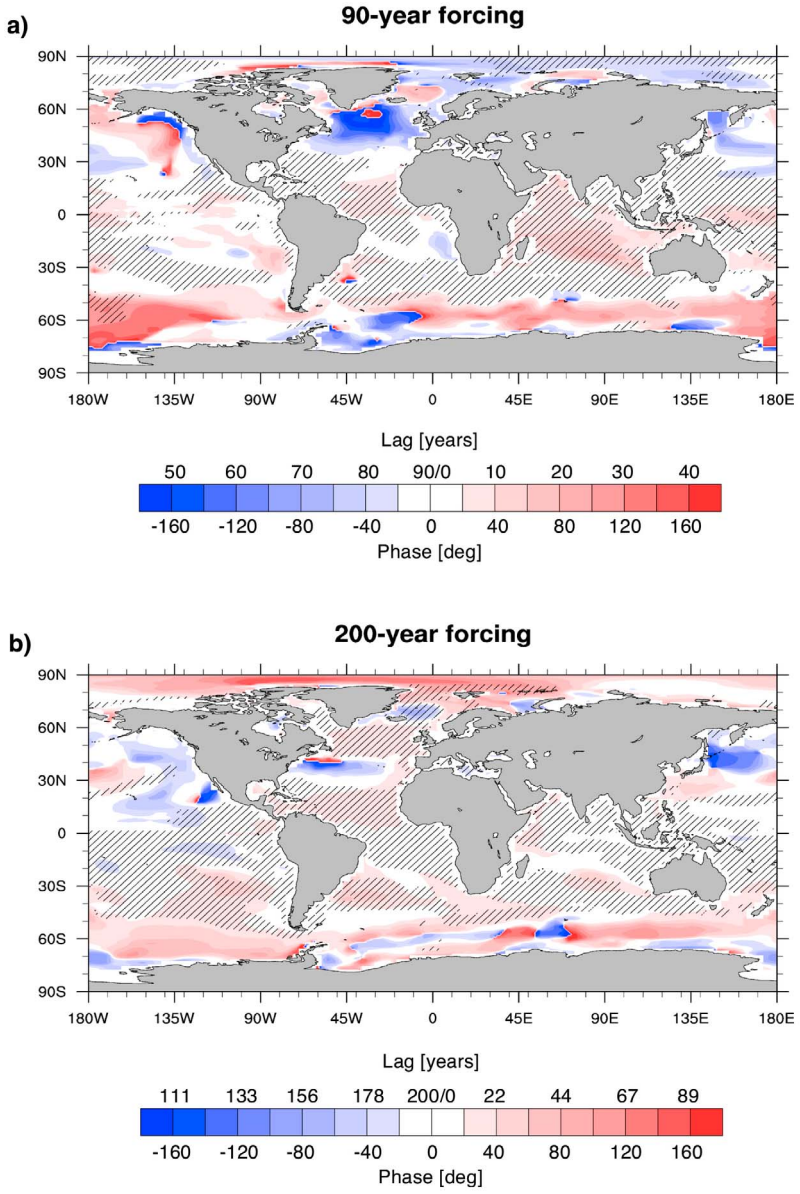

Figure 2. Phase angle (degrees) and lag (years) of ocean potential temperature to idealized TSI forcing at the surface for (a) the 90-year forcing period, and (b) the 200-year forcing period. We assume that at each point changes in TSI lead the variations in temperature (see Section 2). Hatching indicates significant coherency at the 95% level (cf. Figure 1).

forcing period in each experiment. Negative phase angles, which result from the wrapping of $\phi > 180°$ into the interval $[-180°; +180°]$, are corrected by making the physically plausible assumption that at each point changes in TSI lead temperature variations. Cross-spectral analysis is based on smoothed periodograms using a Daniell filter. Initially, time series were tapered, linearly detrended, and had the mean subtracted using the corresponding routines of the NCAR Command Language (NCL) package, version 6.0.0 of *Brown et al.* [2012].

3. Results

[8] The impact of TSI anomalies at the 90-year and 200-year forcing periods on ocean temperature is investigated at the surface, at mid-depth (1112 m) and at deep-water (1884 m) level. For the Atlantic Ocean, the mid-depth level allows for a qualitative comparison with the reconstructed temperature response of *Morley et al.* [2011], while the depth of 1884 m represents North Atlantic Deep Water (NADW) in the model.

[9] Coherency between temperature and solar forcing (Figure 1) yields the spatially most homogeneous response at the surface for both forcing periods, in tropical and subtropical regions, but also at higher latitudes in the Arctic Ocean (90-year forcing) and in the North Atlantic region (200-year forcing). With increasing depth, temperature sensitivity to solar forcing reduces and a pattern of different spatial temperature sensitivity between the two experiments emerges. The 90-year forcing induces a response in the South Atlantic and Southern Indian and Pacific Ocean (1112 m and 1884 m). In contrast, the 200-year experiment exhibits

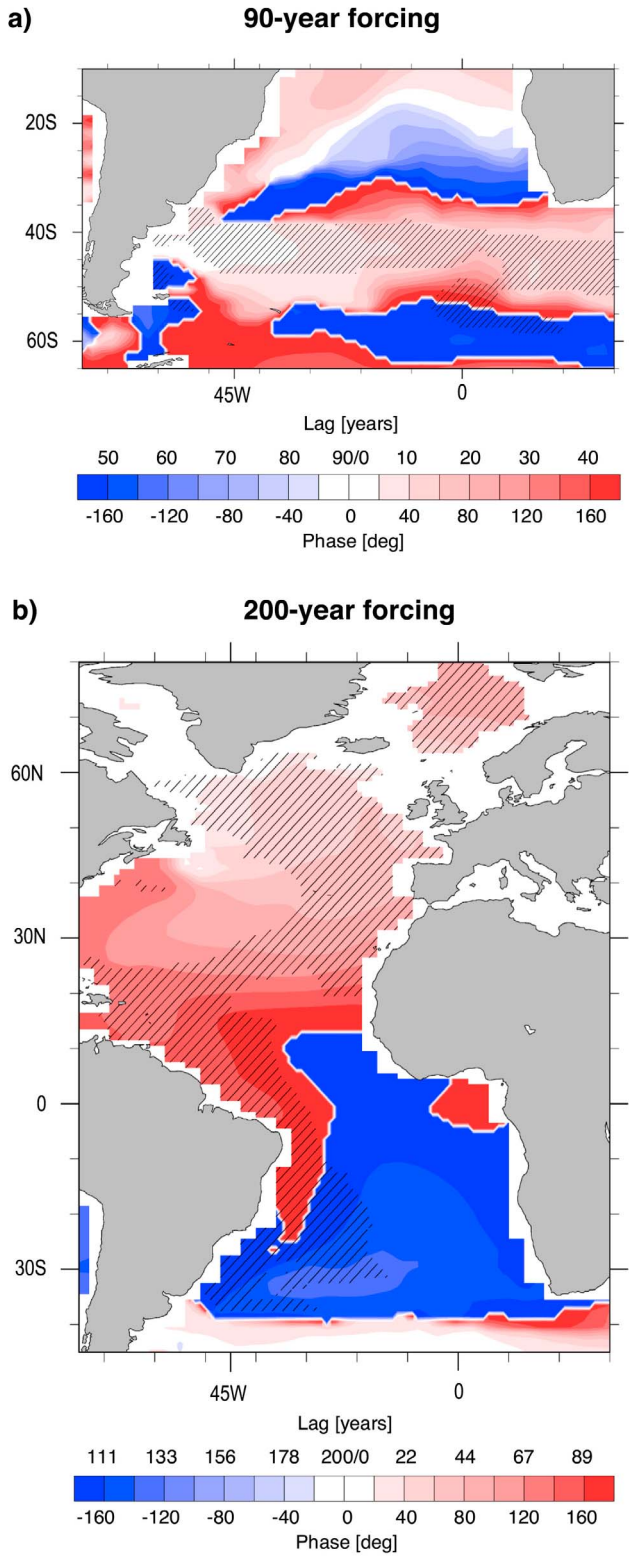

Figure 3. Phase angle (degrees) and lag (years) of ocean potential temperature to idealized TSI forcing at 1884 m depth for (a) the 90-year forcing period, and (b) the 200-year forcing period. We assume that at each point changes in TSI lead the variations in temperature (see Section 2). Hatching indicates significant coherency at the 95% confidence level (cf. Figure 1).

a significant temperature response in the North Atlantic and subtropical South Pacific at mid-depth (1112 m), and nearly the entire Atlantic and Arctic Ocean at the deep level (1884 m).

4. Discussion

[10] Despite the fact that the two forcing periods differ only by a factor of approximately two, the response patterns in the oceanic interior differ significantly between the experiments (Figure 1). To gain further insight into this unexpected result, we turn to the phase lag of the temperature response to TSI forcing in order to deduce mechanisms of signal propagation in the oceanic interior. We limit the interpretation to regions for which the coherency between TSI and temperature is significant at the 95% confidence level.

[11] The surface-temperature response to the idealized TSI forcing (Figure 2) occurs within 20 years and 44 years for the 90-year and 200-year forcing, respectively. Moreover, the two experiments reveal a positive correlation between sea-surface temperature and TSI (not shown). Together with the small lag seen in the temperature response, this is consistent with a direct, thermal forcing of the sea surface in accordance with previous findings [e.g., *Swingedouw et al.*, 2011].

[12] At depth, the temperature lag to TSI forcing is compared between the two experiments at 1884 m (Figure 3). Given the pronounced response especially in the Atlantic Ocean at this depth, we focus on this region for the lag analysis.

[13] In the 90-year forcing experiment, the temperature response is visible as a zonal band at approximately 40°–50°S in the South Atlantic (cf. Figure 1). The lag associated with this response is short ($\phi < 80°$ or $\tau < 20$ yrs; Figure 3a). *Varma et al.* [2011] noted a latitudinal shift in Southern Hemisphere westerly winds in this latitude band in response to solar irradiance variations based on sensitivity experiments with the same climate model and resolution. Accordingly, centennial-scale intervals of higher solar activity were associated with a poleward shift in the westerly winds, and *vice versa* during solar minima. Our experiment reveals a small positive correlation of potential temperature with TSI anomalies (slope $\sim$0.1°C/(Wm^{-2}); not shown) in this region at the deep-water level as well as at the surface. This implies a wind-induced latitudinal shift of the oceanic frontal system at these latitudes, involving a further southward penetration of North Atlantic Deep Water (NADW) during solar maxima, thereby displacing colder Circumpolar Deep Water southward in response to a barotropic adjustment to this shift in wind forcing. A similar feature is visible in the 200-year forcing experiment, albeit not statistically significant (Figure 1b). Neither of the two experiments supports the solar-induced temperature variations at mid-depth in the northeast Atlantic as reconstructed by *Morley et al.* [2011]. We note, however, elevated but statistically insignificant coherency values along the northwest African margin from where the proxy information stems.

[14] The 200-year forcing experiment reveals a gradually increasing lag at 1884 m depth from the northeast Atlantic ($\tau < 30$ years) towards the South Atlantic along the western boundary ($\tau \sim$125 years; Figure 3b), as well as towards the

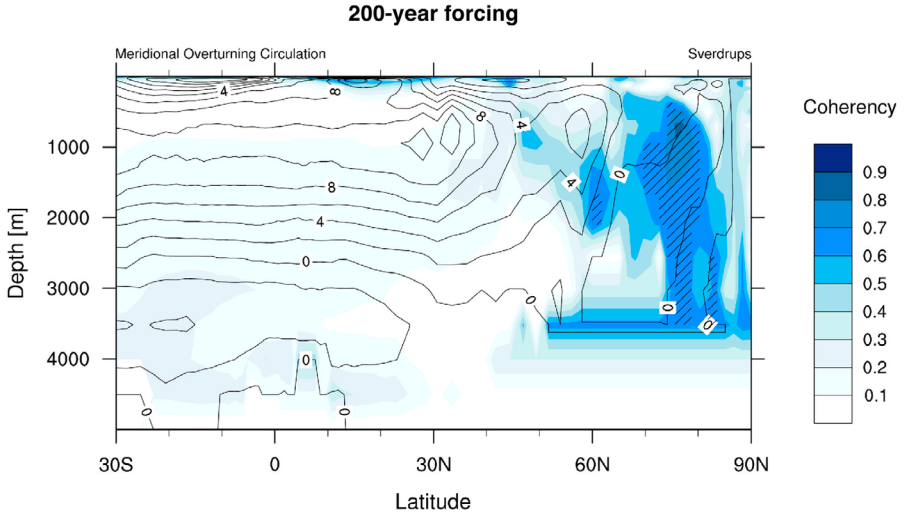

Figure 4. Coherency between the streamfunction of the Atlantic meridional overturning circulation (AMOC) and idealized solar forcing at the 200-year forcing period. Hatching indicates significant coherency at the 95% level. Black contour lines show the long-term mean overturning streamfunction (in units of 10^6 m^3 s^{-1}).

Arctic Ocean (not shown). Previously performed sensitivity experiments with idealized TSI forcing on multi-decadal time scales revealed a sensitivity of the AMOC strength to solar forcing, albeit with a forcing amplitude twice as large as in our experiments (2 Wm^{-2}) [*Park and Latif*, 2012]. Given the spatial pattern of response in the 200-year forcing experiment at 1884 m depth, we investigated the coherency of the AMOC with idealized TSI in this experiment (Figure 4). Significant coherency can be detected at subpolar northern latitudes (ca. 60°–80°N), reaching a depth of ~3600 m. However, the southward component of the meridional overturning stream function at depth does not show any significant response to the TSI forcing. The pattern of increasing temperature lag at the deep level (1884 m) nevertheless indicates a propagation of solar anomalies with the deep western boundary current, taking into account that the clock-wise circulation pattern in the deep North Atlantic (cf. Figure 3b) is due to a shortcoming in the model simulation of the deep western boundary current in this region [cf. *Prange*, 2008]. Thus, the solar signal becomes entrained into the NADW by deep convection and is subsequently propagated towards the South Atlantic via the deep western boundary current without involving any changes in the strength of the meridional overturning circulation. Given the discrepancy with the sensitivity seen in the AMOC strength when forced with a twice-as-large TSI amplitude [*Park and Latif*, 2012], we note that our experiments results may yield a qualitatively different response pattern when excited by a different forcing amplitude. However, investigating this aspect is beyond the scope of our study.

[15] Recent simulations of the surface-climate response to the 11-year solar cycle [*Meehl et al.*, 2009; *Bal et al.*, 2011], including detailed representations of the stratosphere and the stratospheric ozone response to ultraviolet irradiance variations, have resulted in a better match with observed climate anomalies as compared to the sole dependence on TSI forcing. Despite the fact that the stratosphere is only poorly represented in the present experiments, the obtained results are nevertheless promising as a similar model set-up (i.e., TSI forcing of CCSM3) was largely successful in simulating the surface-climate response to solar variability, albeit with lower amplitude [*Meehl et al.*, 2008].

5. Conclusions

[16] Our experiments with idealized TSI forcing suggest a significant sensitivity of ocean temperature down to a depth of at least 1884 m at both forcing periods. Especially at depth, the spatial expression of the temperature response differs between the two experiments. While the 90-year forcing induces a significant temperature response in the mid-depth (1112 m) and deep (1884 m) South Atlantic (~40°–50°S), the 200-year forcing reveals the highest sensitivity to solar-irradiance changes in the northeast Atlantic at mid-depth (1112 m), and nearly the entire Atlantic and Arctic Ocean at the deep-water level (1884 m). Accordingly, different mechanisms of solar signal propagation are proposed for the two experiments, which involve barotropic adjustment in response to shifting westerlies in the South Atlantic when forced with the 90-year period in TSI, and southward advection by NADW in the 200-year-forcing scenario. The previously detected solar-induced temperature anomalies in the northeast Atlantic at the multi-decadal time scale during the late Holocene derived from a proxy-based reconstruction could not unambiguously be confirmed by our experiments. Furthermore, future work is required to more accurately estimate the climatic response to solar variability using models with a properly resolved stratosphere, as has recently been suggested to be important on the 11-year time scale. Our sensitivity analysis could not confirm the sensitivity in AMOC strength to TSI forcing in previous experiments with idealized solar forcing using a forcing amplitude twice as high as the present simulations. Consequently, our findings illustrate the importance to systematically evaluate the role of the forcing amplitude in numerical experiments in triggering different mechanisms of solar signal propagation in the ocean.

[17] **Acknowledgments.** We thank Dennis Shea (NCAR, Boulder, Colorado) for providing details on the cross-spectral analysis procedure of the NCL routines, as well as Ute Merkel (MARUM) for stimulating discussions on the topic. The CCSM3 model experiments were run on the SGI Altix Supercomputer of the "Norddeutscher Verbund für Hoch- und Höchstleistungsrechnen" (HLRN). We are grateful to the two anonymous referees for their very constructive comments.

[18] The Editor thanks two anonymous reviewers for their assistance in evaluating this paper.

References

Ammann, C. M., F. Joos, D. Schimel, B. L. Otto-Bliesner, and R. Tomas (2007), Solar influence on climate during the past millennium: Results from transient simulations with the NCAR Climate System Model, *Proc. Natl. Acad. Sci. U. S. A.*, *104*(10), 3713–3718, doi:10.1073/pnas.0605064103.

Bal, S., S. Schimanke, T. Spangehl, and U. Cubasch (2011), On the robustness of the solar cycle signal in the Pacific region, *Geophys. Res. Lett.*, *38*, L14809, doi:10.1029/2011GL047964.

Bond, G., B. Kromer, J. Beer, R. Muscheler, M. N. Evans, W. Showers, S. Hoffmann, R. Lotti-Bond, I. Hajdas, and G. Bonani (2001), Persistent solar influence on North Atlantic climate during the Holocene, *Science*, *294*, 2130–2136, doi:10.1126/science.1065680.

Braconnot, P., et al. (2007), Results of PMIP2 coupled simulations of the Mid-Holocene and Last Glacial maximum—Part 1: Experiments and large-scale features, *Clim. Past*, *3*, 261–277, doi:10.5194/cp-3-261-2007.

Brown, D., R. Brownrigg, M. Haley, and W. Huang (2012), NCAR Command Language (Version 6.0.0), Natl. Cent. for Atmos. Res., Univ. Corp. for Atmos. Res., Boulder, Colo., doi:10.5065/D6WD3XH5.

Collins, W. D., et al. (2006), The Community Climate System Model Version 3 (CCSM3), *J. Clim.*, *19*, 2122–2143, doi:10.1175/JCLI3761.1.

Cubasch, U., R. Voss, G. C. Hegerl, J. Waszkewitz, and T. J. Crowley (1997), Simulation of the influence of solar radiation variations on the global climate with an ocean-atmosphere general circulation model, *Clim. Dyn.*, *13*, 757–767, doi:10.1007/s003820050196.

Gray, L. J., et al. (2010), Solar influences on climate, *Rev. Geophys.*, *48*, RG4001, doi:10.1029/2009RG000282.

Jiang, H., J. Eiriksson, M. Schulz, K.-L. Knudsen, and M.-S. Seidenkrantz (2005), Evidence for solar forcing of sea-surface temperature on the North Icelandic Shelf during the late Holocene, *Geology*, *33*, 73–76, doi:10.1130/G21130.1.

Knudsen, M. F., P. Riisager, B. H. Jacobsen, R. Muscheler, I. Snowball, and M.-S. Seidenkrantz (2009), Taking the pulse of the Sun during the Holocene by joint analysis of ^{14}C and ^{10}Be, *Geophys. Res. Lett.*, *36*, L16701, doi:10.1029/2009GL039439.

Krivova, N. A., S. K. Solanki, and Y. C. Unruh (2011), Towards a long-term record of solar total and spectral irradiance, *J. Atmos. Sol. Terr. Phys.*, *73*, 223–234, doi:10.1016/j.jastp.2009.11.013.

Lockwood, M. (2011), Shining a light on solar impacts, *Nat. Clim. Change*, *1*, 98–99, doi:10.1038/nclimate1096.

Ma, L. H. (2009), Gleissberg cycle of solar activity over the last 7000 years, *New Astron.*, *14*, 1–3, doi:10.1016/j.newast.2008.04.001.

Meehl, G. A., J. M. Arblaster, G. W. Branstator, and H. van Loon (2008), A coupled air-sea response mechanism to solar forcing in the Pacific region, *J. Clim.*, *21*, 2883–2897, doi:10.1175/2007JCLI1776.1.

Meehl, G. A., J. M. Arblaster, K. Matthes, F. Sassi, and H. van Loon (2009), Amplifying the Pacific climate system response to a small 11-year solar cycle forcing, *Science*, *325*(5944), 1114–1118, doi:10.1126/science.1172872.

Morley, A., M. Schulz, Y. Rosenthal, S. Mulitza, A. Paul, and C. Rühlemann (2011), Solar modulation of North Atlantic central water formation at multi-decadal timescales during the late Holocene, *Earth Planet. Sci. Lett.*, *308*, 161–171, doi:10.1016/j.epsl.2011.05.043.

Park, W., and M. Latif (2012), Atlantic meridional overturning circulation response to idealized external forcing, *Clim. Dyn.*, *39*, 1709–1726, doi:10.1007/s00382-011-1212-0.

Prange, M. (2008), The low resolution CCSM2 revisited: New adjustments and a present-day control run, *Ocean Sci.*, *4*, 151–181, doi:10.5194/os-4-151-2008.

Shindell, D. T., G. A. Schmidt, R. L. Miller, and D. Rind (2001), Northern Hemisphere winter climate response to greenhouse gas, ozone, solar, and volcanic forcing, *J. Geophys. Res.*, *106*, 7193–7210, doi:10.1029/2000JD900547.

Steinhilber, F., J. Beer, and C. Fröhlich (2009), Total solar irradiance during the Holocene, *Geophys. Res. Lett.*, *36*, L19704, doi:10.1029/2009GL040142.

Swingedouw, D., L. Terray, C. Cassou, A. Voldoire, D. Salas-Mélia, and J. Servonnat (2011), Natural forcing of climate during the last millenium: Fingerprint of solar variability. Low frequency solar forcing and NAO, *Clim. Dyn.*, *36*, 1349–1364, doi:10.1007/s00382-010-0803-5.

Varma, V., M. Prange, F. Lamy, U. Merkel, and M. Schulz (2011), Solar-forced shifts of the Southern Hemisphere westerlies during the Holocene, *Clim. Past*, *7*, 339–347, doi:10.5194/cp-7-339-2011.

Wang, Y., H. Cheng, R. L. Edwards, Y. He, X. Kong, Z. An, J. Wu, M. J. Kelly, C. A. Dykoski, and X. Li (2005), The Holocene Asian monsoon: Links to solar changes and North Atlantic climate, *Science*, *308*, 854–857, doi:10.1126/science.1106296.

Weber, S. L., T. J. Crowley, and G. van der Schrier (2004), Solar irradiance forcing of centennial climate variability during the Holocene, *Clim. Dyn.*, *22*, 539–553, doi:10.1007/s00382-004-0396-y.

Yeager, S. G., C. A. Shields, W. G. Large, and J. J. Hack (2006), The low-resolution CCSM3, *J. Clim.*, *19*, 2545–2566, doi:10.1175/JCLI3744.1.